

Dense gas in nearby galaxies

XV. Hot ammonia in NGC 253, Maffei 2 and IC 342

R. Mauersberger¹, C. Henkel², A. Weiß^{1,3}, A.B. Peck^{2,4}, and Y. Hagiwara^{2,5}

¹ Instituto de Radioastronomía Milimétrica (IRAM), Avda. Divina Pastora 7NC, E-18012 Granada, Spain

² Max-Planck-Institut für Radioastronomie, Auf dem Hügel 71, D-53121 Bonn, Germany

³ Radioastronomisches Institut der Universität Bonn, Auf dem Hügel 69, D-53121 Bonn, Germany

⁴ Smithsonian Submillimeter Array (SMA), PO Box 824, Hilo, HI 96721, USA

⁵ ASTRON, Westerbork Observatory, P.O. Box 2, 7990AA Dwingeloo, The Netherlands

Received ; accepted

Abstract. The detection of NH₃ inversion lines up to the $(J, K) = (6, 6)$ level is reported toward the central regions of the nearby galaxies NGC 253, Maffei 2, and IC 342. The observed lines are up to 406 K (for $(J, K) = (6, 6)$) and 848 K (for the $(9, 9)$ transition) above the ground state and reveal a warm ($T_{\text{kin}} = 100 \dots 140$ K) molecular component toward all galaxies studied. The tentatively detected $(J, K) = (9, 9)$ line is evidence for an even warmer (> 400 K) component toward IC 342. Toward NGC 253, IC 342 and Maffei 2 the global beam averaged NH₃ abundances are $1 - 2 \cdot 10^{-8}$, while the abundance relative to *warm* H₂ is around 10^{-7} . The temperatures and NH₃ abundances are similar to values found for the Galactic central region. C-shocks produced in cloud-cloud collisions can explain kinetic temperatures and chemical abundances. In the central region of M 82, however, the NH₃ emitting gas component is comparatively cool (~ 30 K). It must be dense (to provide sufficient NH₃ excitation) and well shielded from dissociating photons and comprises only a small fraction of the molecular gas mass in M 82. An important molecular component, which is warm and tenuous and characterized by a low ammonia abundance, can be seen mainly in CO. Photon dominated regions (PDRs) can explain both the high fraction of warm H₂ in M 82 and the observed chemical abundances.

Key words. Galaxies: individual: NGC 253, Maffei 2, IC 342, M 82 – Galaxies: ISM – Galaxies: starburst – Galaxies: abundances – Radio lines: galaxies

1. Introduction

Many galaxies, including our own, show large concentrations of molecular gas in their central few hundred parsecs. Due to the presence of bars facilitating inflow of gas, this material is often originating from further out. Reaching the nuclear region, the gas may trigger bursts of star formation and the formation of an active nucleus. There have been many studies to determine the distribution and kinematics of this gas, mainly using the mm-wave transitions of CO as a tracer of the more elusive H₂ (see e.g. Combes 1991, Young & Scoville 1991).

In the Galactic disk, there is a well established linear correlation between the integrated CO intensity, I_{CO} , and H₂ (see Sect. 4.2 for a discussion and references). It has become evident, however, that the relationship is different in the central regions of galaxies (e.g. Downes et al. 1992, Sodroski et al. 1995, Mauersberger et al. 1996a, 1996b, Dahmen et al. 1998).

Even more difficult is the determination of local physical parameters, such as density and kinetic temperature of the gas. The difficulties compared to similar studies of nearby clouds in the galactic disk have two main reasons: Firstly, lines of extragalactic density or temperature tracers, i.e. molecules with a high dipole moment such as CS, HC₃N, or NH₃, are broad and weak; they require high quality baselines and good sensitivity. Secondly, a low linear resolution forces us to average over regions of several 100 pc. Area filling factors are not well known but are certainly less than unity and it becomes difficult to disentangle the different gas components which certainly coexist within one telescope beam.

Nevertheless, there has been progress in determining physical parameters toward the nuclear regions of nearby galaxies. The most prominent examples are NGC 253, M 82, NGC 4945 and IC 342. These and other galaxies have been mapped with high resolution in the line emission of high density tracing molecular transitions (e.g. Downes et al. 1992, Brouillet & Schilke 1993, Paglione et

al. 1995, Peng et al. 1996). Multilevel studies in CS, HCN, HCO⁺, CH₃CN, CH₃CCH, CH₃OH, H₂CO and HC₃N were carried out to determine H₂ densities, $n(\text{H}_2)$, toward some of those galaxies (Mauersberger et al. 1989, 1990, 1991, Walker et al. 1993, Jackson et al. 1995, Hüttemeister et al. 1997, Paglione et al. 1997, Seaquist et al. 1998, Schulz et al. 2001). The level populations of such molecules depend on their spontaneous deexcitation rates and on the frequency of collisions with H₂, i.e. mostly on the H₂ density, and to a lesser degree on the kinetic temperature of the gas. From these studies of high density tracers we have obtained a good idea of $N(\text{H}_2)$ in components with $n(\text{H}_2)$ ranging between 10^4 and several 10^5 cm^{-3} . In order not to miss the less dense and more extended gas, studies of CO in its various transitions across the mm, sub-mm and FIR range were also carried out (e.g. Güsten et al. 1993, Mao et al. 2000, Schulz et al. 2001, Ward et al. 2001, Bradford et al. 2002).

One of the less well known parameters has been the gas kinetic temperature. With area filling factors that are not known, a thermalized low density tracer like CO cannot be used to determine T_{kin} in extragalactic sources. Alternative thermometers for the extragalactic molecular medium are symmetric top molecules where relative level populations are determined predominantly by collisions (and to a lesser degree by spontaneous radiation), such as NH₃ or CH₃CN. Temperatures in excess of 200 K have been obtained for clouds near our Galactic center (Mauersberger et al. 1986, Hüttemeister et al. 1993a, 1993b, 1995, Rodríguez-Fernández et al. 2001, Ceccarelli et al. 2002). From a few low energy ammonia lines, kinetic temperatures were determined toward NGC 253 (Takano et al. 2002), Maffei 2 (Henkel et al. 2000), IC 342 (Martin & Ho 1986), and M 82 (Weiß et al. 2001a). However, symmetric top molecules need H₂ densities of order 10^4 cm^{-3} to be excited. Hence they probe a dense gas component which is important for star formation but do not trace the temperature of low density, CO-emitting, molecular gas. For such a low density molecular component, observations of H₂ lines are more significant. Recently, Rigopoulou et al. (2002) concluded from observations of rotational H₂ lines toward a number of starburst and Seyfert galaxies that a significant fraction (up to 10% in starburst galaxies; 2–35% in Seyferts) of the gas in the centers of such galaxies has temperatures in the range of 150 K.

In order to obtain more stringent values for the dense gas and to identify the origin and excitation of this gas we have measured higher energy inversion lines up to 405 K above the ground state toward the central regions of NGC 253, Maffei 2 and up to 848 K toward IC 342. Combined with new CS $J = 5 - 4$ and ¹³CO $J = 2 - 1$ data to trace also density and column density, a dense and warm molecular gas component is revealed in the central regions of these galaxies.

Table 1. Summary of observations

Transition	Telescope	Frequency GHz	θ_{beam} "
NH ₃ (1,1)	MPIfr 100-m	23.694	40
NH ₃ (2,2)	MPIfr 100-m	23.723	40
NH ₃ (3,3)	MPIfr 100-m	23.870	40
NH ₃ (4,4)	MPIfr 100-m	24.139	39
NH ₃ (5,5)	MPIfr 100-m	24.533	39
NH ₃ (6,6)	MPIfr 100-m	25.056	38
NH ₃ (9,9)	MPIfr 100-m	27.478	34
¹³ CO (2 - 1)	HHT 10-m ^a	220.399	34
CS (5 - 4)	HHT 10m ^a	244.936	32

a) in the observed frequency range, the beam efficiency of the HHT is 0.78

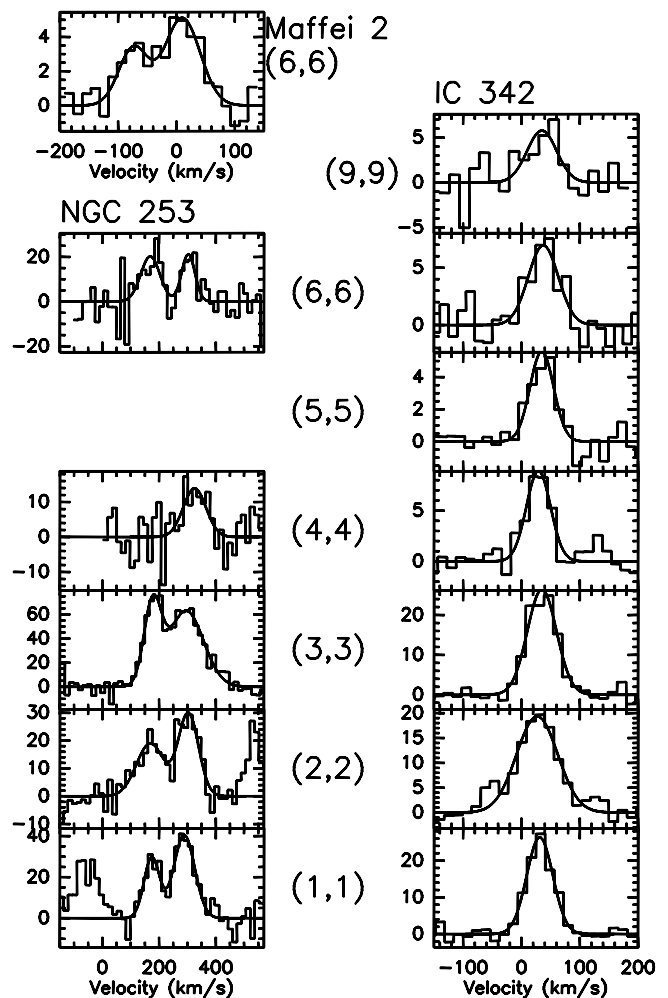


Fig. 1. Ammonia (NH₃) inversion lines (in units of mK, T_{mb}) toward the centers of NGC 253 ($\alpha_{2000} = 0^{\text{h}}47^{\text{m}}33^{\text{s}}.2$, $\delta_{2000} = -25^{\circ}17'16''$), Maffei 2 ($\alpha_{2000} = 2^{\text{h}}41^{\text{m}}55^{\text{s}}.2$, $\delta_{2000} = 59^{\circ}36'11''$) and IC 342 ($\alpha_{2000} = 3^{\text{h}}46^{\text{m}}48^{\text{s}}.6$, $\delta_{2000} = 68^{\circ}05'46''$), measured at Effelsberg. The spectra have been smoothed to a velocity resolution of $\sim 15 \text{ km s}^{-1}$ (17 km s^{-1} for the (9,9) transition). Toward NGC 253, the feature to the left of the (1,1) line is part of the (2,2) profile, and the feature to the right of the (2,2) line is part of the (1,1) profile.

Table 2. NH₃, CS(5 – 4) and ¹³CO (2-1) results

Line	T_{mb} mK	$\int T_{\text{mb}} dv^a$ K km s ⁻¹	v_{LSR}^a km s ⁻¹	Δv^a km s ⁻¹	$N(J, K)^{a,b}$ 10 ¹² cm ⁻²
NGC 253					
NH ₃ (1,1)	29	2.0(.6)	174(10)	64(21)	26(8)
NH ₃ (1,1)	41	3.8(.8)	288(8)	87(22)	50(10)
NH ₃ (2,2)	19	2.3(.7)	169(15)	114(44)	23(7)
NH ₃ (2,2)	29	2.3(.6)	303(10)	84(18)	23(6)
NH ₃ (3,3)	65	5.1(.6)	177(3)	72(6)	45(5)
NH ₃ (3,3)	63	9.7(.8)	295(5)	145(13)	84(7)
NH ₃ (4,4) ^c	14	1.4(.4)	325(13)	95(23)	11.2(3.1)
NH ₃ (6,6)	20	1.7(.5)	<i>169</i>	79(20)	12.9(3.8)
NH ₃ (6,6)	21	1.2(.4)	<i>303</i>	55(18)	9.2(3.0)
CS(5 – 4)	45	7.7(0.9)	215(10)	162(20)	
¹³ CO(2 – 1)	244	52.4(4.3)	251(8.5)	202(19)	
Maffei 2					
NH ₃ (6,6)	3.4	.21(.06)	–74(8)	59(17)	1.5 (.4)
NH ₃ (6,6)	5.1	.39(.06)	10(6)	72(12)	2.8 (.4)
CS(5 – 4)		< 0.5 ^d			
¹³ CO(2 – 1)	6.2	5.2(1.6)	–99(10)	79(16)	
¹³ CO(2 – 1)	6.2	8.7(1.9)	23(14)	132(32)	
IC 342					
NH ₃ (1,1)	26.3	1.5(.07)	31.4(1.2)	52.8(2.8)	20.0(1.0)
NH ₃ (2,2)	19.4	1.7(.10)	26.8(2.2)	83.0(6.7)	16.7(1.0)
NH ₃ (3,3)	26.4	1.7(.06)	35.1(1.1)	58.8(2.3)	14.9(.5)
NH ₃ (4,4)	8.8	.47(.04)	29.1(2.2)	48.9(4.7)	3.8(.3)
NH ₃ (5,5)	5.6	.29(.03)	34.8(2.6)	47.6(6.2)	2.2(.2)
NH ₃ (6,6)	7.0	.45(.06)	37.4(3.7)	60.7(8)	3.2(0.4)
NH ₃ (9,9)	5.8	.34(.08)	<i>35</i>	<i>60</i>	2.1(.5)
CS(5 – 4)	8.5	.78(.17)	<i>30</i>	86(21)	
¹³ CO(2 – 1)	253	17.2(1.1)	24.5(1.9)	64.1(4.5)	
M 82					
CS(5 – 4)	9	1.3(0.3)	150(11)	129(36)	
CS(5 – 4)	17	1.8(0.2)	303(6)	94(13)	
¹³ CO(2 – 1)	100	13.5(1.2)	<i>150</i>	<i>129</i>	
¹³ CO(2 – 1)	150	15.9(1.0)	<i>303</i>	<i>94</i>	

a) values in italics have been fixed in the Gaussian fits, all errors are 1σ

b) total beam averaged column density of the observed (J, K) rotational level including both the upper *and* lower inversion state.

c) (4,4) data toward NGC 253 may be affected by pointing problems (see Sect. 3.1)

d) 1σ upper limit

2. Observations

2.1. Effelsberg Observations of NH₃ lines

Between October 2000 and September 2002, the $(J, K) = (1,1)$ to $(6,6)$ inversion lines of ammonia were observed using the Effelsberg 100-m telescope¹. The observed line frequencies and the corresponding beam sizes are summarized in Table 1.

¹ The 100-m telescope at Effelsberg is operated by the Max-Planck-Institut für Radioastronomie (MPIfR) on behalf of the Max-Planck-Gesellschaft

The data were recorded with a dual channel K-band HEMT receiver with $T_{\text{sys}} \sim 200$ K on a main beam brightness temperature scale (T_{mb}). The measurements were carried out in a dual beam switching mode, with a switching frequency of 1 Hz and a beam throw of 2' in azimuth. An ‘AK 90’ autocorrelator included eight spectrometers with 512 or 256 channels and bandwidths of 40 or 80 MHz each, leading to channel spacings of ~ 1 or 4 km s⁻¹. The eight spectrometers were configured such that the $(J, K) = (1,1)$ to $(4,4)$, $(4,4)$ and $(5,5)$, or $(5,5)$ and $(6,6)$ lines could be observed simultaneously. Data with one individual line, either $(J, K) = (5,5)$ or $(6,6)$, were also taken.

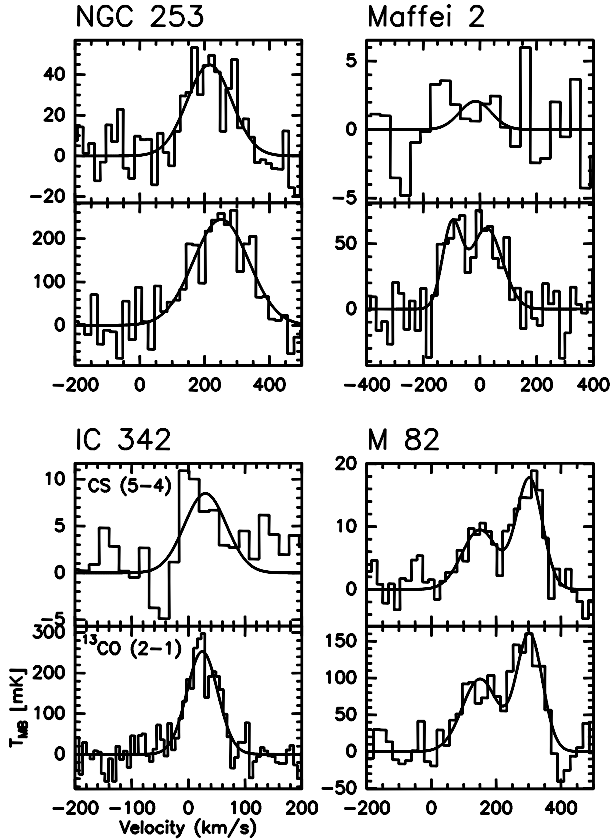


Fig. 2. CS $J=5-4$ and ^{13}CO $J=2-1$ profiles measured with the HHT. For a comparison with NH_3 data from Weiß et al. (2001a) we also include profiles measured toward M 82 ($\alpha_{2000} = 9^{\text{h}}55^{\text{m}}52^{\text{s}}.6$, $\delta_{2000} = 69^{\circ}40'46''$). The velocity resolution has been smoothed to 17 km s^{-1} .

At least two backends were centered on each ammonia line to sample both linear polarizations independently. For NGC 253, only one of the two receiver channels provided useful data.

The (9,9) line at 27.478 GHz was observed in December 1995 using a single channel 1 cm HEMT receiver equipped with a 1024 channel autocorrelator. System temperatures were near 500 K on a T_{mb} scale. The beam size was $34''$. The (9,9) line was measured in a position switching mode with a bandwidth of 25 MHz and a channel spacing of $\sim 0.27 \text{ km s}^{-1}$.

Flux calibration was obtained by regularly observing both the continuum and the ammonia lines of W3(OH) (for fluxes see Mauersberger et al. 1988, Ott et al. 1994). Pointing was checked every hour. W3(OH) was the pointing source for IC 342 and Maffei 2; PKS 0023–26 was used for NGC 253. The pointing accuracy was found to be stable within $5''$ – $10''$.

A linear baseline was removed from each individual spectrum and spectra were added with relative weights

depending on the noise level outside the velocity range of the respective line. We estimate the flux calibration of the final reduced spectra to be accurate within $\pm 15\%$.

2.2. CS and ^{13}CO observations with the Heinrich-Hertz-Telescope

The $J=5-4$ transition of $^{12}\text{C}^{32}\text{S}$ (hereafter CS) and the $J=2-1$ transition of $^{13}\text{C}^{16}\text{O}$ (hereafter ^{13}CO) were observed in November 2001 toward NGC 253, Maffei 2, IC 342, and M 82 using the 10-m Heinrich-Hertz-Telescope² (Baars & Martin 1996). At the line frequencies of 244.9536 GHz (CS) and 220.3987 GHz (^{13}CO), the beam width was $\sim 32''$. The zenith optical depth at 225 GHz as determined by a tipping radiometer was typically 0.2–0.4. A single channel SIS receiver with a total bandwidth of ~ 0.8 GHz tuned in double sideband mode was used for the observations. The spectrometer was a 2048 channel AOS with a channel separation of 0.48 MHz ($\sim 0.6 \text{ km s}^{-1}$). The beam efficiency of the HHT is 0.78 in the observed frequency range. System temperatures were 600–1000 K on a T_{mb} scale. The calibration procedure was described by Mauersberger et al. (1999). The observing mode was symmetric wobbler switching with a throw of $\pm 200''$ in azimuth. The pointing was checked every 3–5 hours and was accurate to $< 5''$. Errors in the calibration procedure, atmospheric fluctuations and deviations from a sideband gain ratio of unity should result in an uncertainty of $\pm 20\%$ in the intensity scale. After co-adding the spectra, we subtracted first order baselines and smoothed to a velocity resolution of $\sim 17 \text{ km s}^{-1}$.

3. Results

3.1. NH_3

The measured spectra are displayed in Fig. 1, and the results of Gaussian fits to the profiles, namely the velocity integrated main-beam brightness temperatures $\int T_{\text{mb}} dv$, the velocities relative to the local standard of rest (v_{LSR}) and the full-width to half power linewidths ($\Delta v_{1/2}$) are summarized in Table 2. For the (9,9) line toward IC 342 we have fixed the central velocity and linewidth in order to reduce the nominal error for the integrated intensity. We have clearly detected the (1,1) ... (6,6) transitions and tentatively also the (9,9) transition toward IC 342, the (1,1) ... (4,4) and (6,6) lines toward NGC 253 and the (6,6) line toward Maffei 2. These are the first detection of the (5,5) transition, the first definite detections of the (6,6) transition and the first tentative detection of an NH_3 (9,9) line outside the Galaxy.

Toward NGC 253, we find two velocity components in the (1,1), (2,2), (3,3) and (6,6) lines at ~ 175 and 290 km s^{-1} , each with a linewidth of 80 – 100 km s^{-1} , which presumably arise from two intensity peaks also seen

² The HHT is operated by the Submillimeter Telescope Observatory on behalf of Steward Observatory and the MPIfR.

in higher resolution maps (Mauersberger et al. 1996a, Harrison et al. 1999). These velocity components cannot be distinguished in our (4,4) profile. As line width and central velocity indicate, this line only shows the 300 km s^{-1} component. Therefore we cannot exclude an exceptionally large pointing error favoring the higher velocity peak. From CO mapping (e.g. Mauersberger et al. 1996a, Dumke et al. 2001) the observed line profile can be reproduced if the telescope was mispointed by $\sim 10''$ toward the SW. Therefore we will not account for the detailed shape of the (4,4) line in the further interpretation of our results but will take the presence of the (4,4) line as just another indication for the presence of warm molecular gas.

For the lower lying transitions of ammonia and other molecules toward Maffei 2, there are two velocity components, at about -80 and $+6 \text{ km s}^{-1}$ (e.g. Henkel et al. 2000), each with a line width of $\sim 50 \text{ km s}^{-1}$. Our (6,6) spectrum is consistent with these results (see Fig. 1 and Table 1). A single velocity component could fit all data from IC 342.

3.2. CS (5 – 4) and ^{13}CO (2 – 1)

We have detected CS (5 – 4) emission toward NGC 253, IC 342, and M 82. Toward Maffei 2, we obtain an upper limit. ^{13}CO emission was observed toward all four galaxies. The profiles are shown in Fig. 2 and results from Gaussian fits are presented in Table 2.

3.3. Source structure, beam size and line intensities

To constrain molecular abundances and physical conditions from observed CS line intensities, it is crucial that the transitions are observed with comparable beam sizes or that appropriate corrections are applied accounting for beam size and source morphology. Not included in this discussion is Maffei 2 for which not enough CS data exist. For IC 342 we have assumed that the observed CS and NH_3 emission arises from the same volume as the ^{13}CO $J=1-0$ emission that was observed with high spatial resolution by Meier et al. (2000). Smoothing the ^{13}CO $J=1-0$ data cube to different beam sizes thus enables us to investigate the dependence of observed line intensity on the beam size. The same procedure was applied to the distribution of the molecular gas in M 82 using the high angular resolution C^{18}O $J=1-0$ map of Weiss et al. (2001b) and to NGC 253, using the distribution of CS $J=2-1$ (Peng et al. 1996). The CS line intensities expected at $32''$ resolution (the beam size of our CS $J=5-4$ data, see Sect. 2.2) are summarized in Table 3. Given the uncertainties of the latter approximation and accounting for possible differences between the C^{18}O or ^{13}CO versus the CS distributions in M 82 and IC 342, we estimate an error of $\pm 30\%$ for the intensity of individual CS lines convolved to a beam size of $32''$.

Table 3. CS peak line intensities in main beam brightness temperature (mK) at $32''$ resolution, the HHT CS $J=5-4$ beam size. Estimated errors are $\pm 30\%$ (see Sect. 3.3).

Transition	NGC 253	IC 342	M 82 (SW)
CS $J=2-1$	160 ^a	80 ^a	92 ^d
CS $J=3-2$	77 ^a	45 ^{a,e}	34 ^a
CS $J=5-4$	50 ^a , 45 ^b	12 ^a , 8.5 ^b	13 ^{b,e}
C^{34}S $J=2-1$	23 ^a	12 ^{c,f}	14 ^a
C^{34}S $J=3-2$	–	8 ^{c,f}	4 ^a

a) original data from Mauersberger & Henkel (1989)

b) this paper

c) original data from Mauersberger et al. (1995)

d) original data from Baan et al. (1989)

e) data measured with $0''$, $+10''$ offset to other lines

f) data measured with $0''$, $-10''$ offset to other lines

4. Discussion

In the following, we discuss the nuclear regions of all four galaxies observed in the ^{13}CO $J=2-1$ and CS $J=5-4$ transitions, i.e. NGC 253, Maffei 2, IC 342, and M 82 (see Fig. 2). NH_3 data from M 82 will be taken from Weiß et al. (2001a). The NH_3 observations (Fig. 1, Weiß et al. 2001a) will be used to derive kinetic temperatures in regions dense enough ($\gtrsim 10^4 \text{ cm}^{-3}$) to excite the NH_3 inversion lines. The ^{13}CO observations are needed to estimate H_2 column densities and the CS data will be used to determine $n(\text{H}_2)$ densities, CS column densities, and CS abundances relative to H_2 .

4.1. NH_3 column densities and rotational temperatures

In the optically thin case, the beam averaged column density of a rotational state of ammonia (i.e. upper plus lower inversion level) is related to the velocity integrated main-beam brightness temperature by

$$N(J, K) = \frac{1.55 \cdot 10^{14} \text{ cm}^{-2}}{\nu} \frac{J(J+1)}{K^2} \int T_{\text{mb}} dv, \quad (1)$$

with ν being the line frequency in GHz, and $\int T_{\text{mb}} dv$ being the integrated intensity in K km s^{-1} . Here we assumed that the excitation temperature of the inversion lines is $> 1\text{K}$, the energy difference of the two states of a given (J, K) level. The calculated total column densities and their errors are displayed in Table 2. Because most lines were measured simultaneously, the main contribution to the given uncertainties arises from the errors in the Gaussian fits.

If one plots $\log_{10}(N(J, K)/(g_{\text{op}}(2J+1)))$, where $g_{\text{op}} = 2$ for ortho-ammonia ($K = 3, 6, 9, \dots$) and 1 for para-ammonia ($K = 1, 2, 4, 5, 7, \dots$), against the energy of the involved (J, K) rotational state, the slope of a linear fit to two or more rotational levels, m , is related to a rotational temperature (T_{rot}) by $T_{\text{rot}} = -0.434/m$ (e.g. Mauersberger et al. 1986). Such rotational diagrams (Boltzmann plots) are displayed in Fig. 3 for the observed galaxies. For NGC 253, a Boltzmann plot is given for each

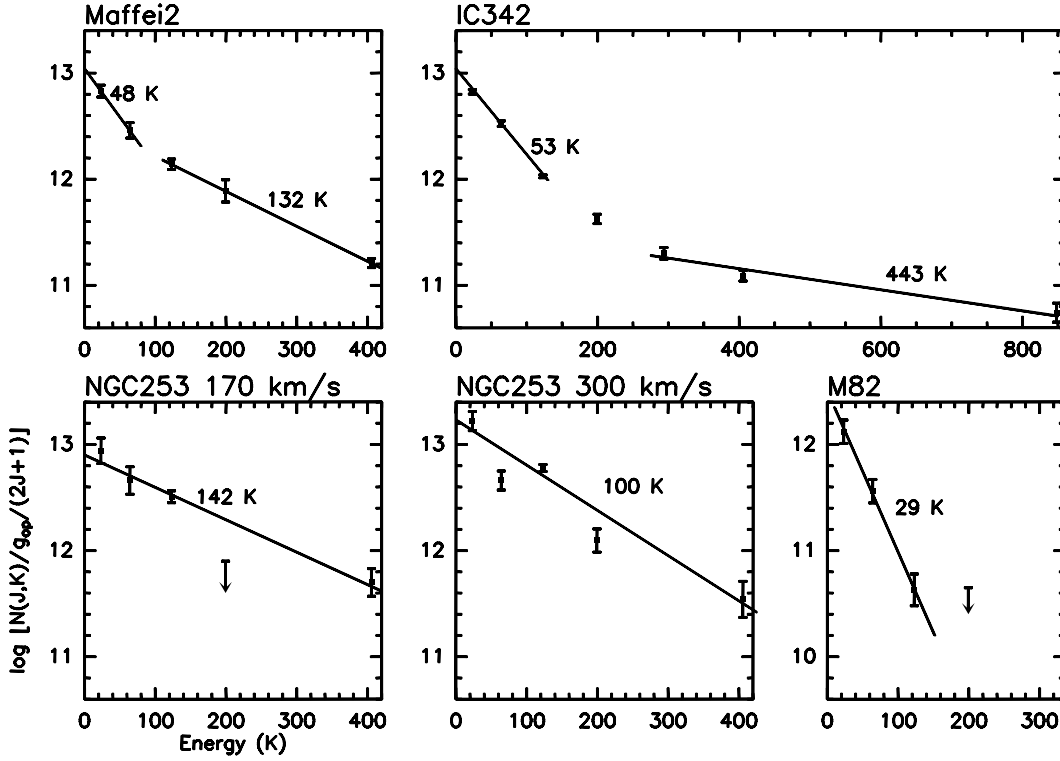


Fig. 3. A Boltzmann plot for the metastable NH_3 levels (i.e. with $J = K$) observed toward Maffei 2 (data for $(J, K) < (6, 6)$ are from Henkel et al. 2000), for IC 342 and for the two velocity components of NGC 253 at 170 and 300 km s^{-1} . We also show the M82 data from Weiß et al. (2001a) correcting an error in the position of the (4,4) limit in their paper. The x-axis denotes the energy level of the corresponding rotational transition in K, the y-axis denotes $\log(N(J, K)/g_{\text{op}}(2J+1))$ (see Sect. 4.1). For a better comparison of the resulting temperatures, the scales in all frames and axes are the same. Linear regressions to the data and the resulting values for T_{rot} are shown.

of the two observed velocity components. Column densities for Maffei 2 have been calculated from the data in Henkel et al. (2000).

Fig. 3 shows the first extragalactic Boltzmann plots from ammonia with fits extending beyond the (4,4) line (energy level: 199 K) to energies of 405 K and 848 K. Table 4 summarizes data for the central regions of the galaxies discussed in more detail below. Model calculations (e.g. Walmsley & Ungerechts 1983) indicate that due to collisional deexcitation of metastable levels (i.e. with $J = K$) via lower lying metastable levels the rotational temperature is only a lower limit to the gas kinetic temperature. This effect is less pronounced for the higher metastable ammonia lines, which therefore should be a more reliable indicator of kinetic temperatures.

4.1.1. Comments on individual sources

NGC 253. For NGC 253, the (4,4) line has not been included in the fit (see Sect. 3.1). We show fits for two velocity components, each corresponding to one of the twin peaks separated symmetrically by about $10''$ from the center of NGC 253 (Mauersberger et al. 1996a). The data can be fitted by a single rotational temperature of $142(\pm 14)$ K for the 170 km s^{-1} component and $100(\pm 3)$ K for the 300 km s^{-1} component. These values are much

higher than the rotational temperature of 17–50 K derived from measurements of the (1,1) to (3,3) lines and a non-detection of the (4,4) line by Takano et al. (2002). Ortho to para ammonia abundance ratios of up to 6 have been claimed by Takano et al. (2002) for some velocity components toward NGC 253. Such a high ratio would indicate that NH_3 was formed in a very cold (< 10 K) environment. Although the (3,3) line seems to be stronger than expected from the intensities of the (2,2) and (4,4) lines, the (6,6) line (which also belongs to the ortho species) has a normal intensity. We therefore cannot confirm an anomalous ortho-to-para ratio in NGC 253. Unlike in Maffei 2 and IC 342 (see below), in NGC 253 we cannot identify an important amount of cool (< 50 K) in ammonia. In Sect. 4.4 we argue that this is due to an elevated relative abundance of NH_3 in the warm component.

If we assume a thermalization at those temperatures and further assume that the non-metastable ammonia levels (i.e. those with $J > K$) are not populated (a reasonable assumption because a significant population would require $n(\text{H}_2) > 10^6 \text{ cm}^{-3}$, e.g. Mauersberger et al. 1985), the total ammonia column densities obtained are $1.6 \cdot 10^{14} \text{ cm}^{-2}$ for the 170 km s^{-1} and $2.1 \cdot 10^{14} \text{ cm}^{-2}$ for the 300 km s^{-1} component.

Maffei 2. As toward NGC 253, two velocity components are detected in Maffei 2. While Henkel et al. (2000) suggested that the -80 km s^{-1} component shows higher excitation than the $+6 \text{ km s}^{-1}$ feature, our (6,6) line spectrum (Fig. 1) indicates equal excitation within the limits of observational accuracy. A single rotational temperature does not yield a good fit to the data. The (1,1) and (2,2) lines can be fitted by $T_{\text{rot}} = 48(\pm 15) \text{ K}$ and the (3,3) to (6,6) lines by $T_{\text{rot}} = 132(\pm 12) \text{ K}$. In a previous study, Takano et al. (2000) derived from a stronger than expected (3,3) line of ortho-ammonia an anomalously high ortho/para ratio of 2.6 for ammonia, which would be an indication of NH_3 formation in a cold (13 K) environment. Our higher signal-to-noise (4,4) and (6,6) data do not support this finding: the ortho/para ratio toward Maffei 2 is normal. Assuming that the (0,0) rotational level is connected to the (1,1) and (2,2) levels by a rotational temperature of 48 K, the total ammonia column density in all metastable levels is $8.6(1.3) 10^{13} \text{ cm}^{-2}$.

IC 342. There is no single rotational temperature for all the observed lines. The (1,1) ... (3,3) transitions can be represented by $T_{\text{rot}} = 53(\pm 1) \text{ K}$ and the (5,5) ... (9,9) lines by $T_{\text{rot}} = 443(\pm 130) \text{ K}$. If we had not included the (9,9) data, the temperatures obtained would have been similar to those obtained for NGC 253. Assuming that the (0,0) rotational level is connected to the (1,1) ... (3,3) levels by a rotational temperature of 53 K, the total ammonia column density in all metastable levels is $7.5(0.5) 10^{13} \text{ cm}^{-2}$. About 1/3 of this total column belongs to a hot component of several 100 K.

M82. Although we are adding no new ammonia data to those observed by Weiß et al. (2001a), we notice that in their Boltzmann plot the limit for the (4,4) line was erroneously plotted too low. While the (1,1) ... (3,3) lines can be described by a common temperature of $29(\pm 1) \text{ K}$, the (4,4) line's upper limit cannot exclude that the higher ammonia levels are described by components with high rotational temperature, like in other galaxies observed.

4.2. Determining $N(\text{H}_2)$ from ^{13}CO

The integrated intensity of $^{12}\text{CO } 1-0$ has been empirically related to the H_2 column density for Galactic disk molecular clouds (e.g. Dickman 1975, Sanders et al. 1985, Bloemen et al. 1986). The theoretical explanation of such a universal X -factor requires three conditions to be fulfilled (Dickman et al. 1986, Mauersberger & Henkel 1993), namely that (a) there are many unresolved clouds with optically thick CO emission within a beam (CO counts clouds), (b) that these clouds are in virial equilibrium and (c) that the CO rotational levels are populated via collisions with H_2 molecules. For molecular clouds near galactic centers (including our own), conditions a) and c) are likely fulfilled. It is, however, by no means clear whether molecular clouds close to the central regions of

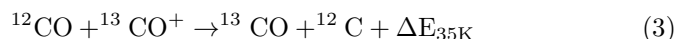
galaxies are virialized (except perhaps the very densest regions). Tidal forces from the nuclear regions or high stellar densities may easily rival the proper gravitational forces of a molecular cloud near a galactic center (e.g. Güsten 1989, Mauersberger et al. 1996a). For such tidally disturbed clouds, the theoretical explanation of the X factor, which works so well for molecular clouds in the Galactic disk, would not be valid anymore. This is even more true for any molecular intercloud medium (e.g. Downes et al. 1992, Jog & Das 1993, Solomon et al. 1997, Downes & Solomon 1998), which is certainly not virialized. An increasing number of examples reveal that the same X factor from the Galactic disk cannot be used near the centers of galaxies (Galactic Center: Sodroski et al. 1995, Dahmen et al. 1998, NGC 253: Mauersberger et al. 1996a, NGC 4945: Mauersberger et al. 1996b, M 82: Mao et al. 2000, Weiß et al. 2001b, ultraluminous galaxies: Solomon et al. 1997).

Relating optically thin transitions of CO to the H_2 column density requires far fewer assumptions than for optically thick ^{12}CO transitions. The mm-transitions of $^{12}\text{C}^{18}\text{O}$ (hereafter C^{18}O) are in most conceivable cases of astrophysical interest optically thin (e.g. Mauersberger et al. 1992); the transitions of ^{13}CO should be in most cases optically thin or only moderately optically thick. Because of the high chemical stability of CO and its isotopes their relative chemical abundance should vary less than that of other molecules in the interstellar medium. Model calculations (Mauersberger et al. 1992) show that for a large range of temperatures and densities the intensity $I = \int T_{\text{mb}} dv$ (in K km s^{-1}) of an optically thin isotopic CO ($^i\text{C}^j\text{O}$) $J = 2 - 1$ line is related to the H_2 column density by

$$N(\text{H}_2) = 5.3 10^{14} \text{ cm}^{-2} \left(\frac{[^i\text{C}^j\text{O}]}{[\text{H}_2]} \right)^{-1} I(^i\text{C}^j\text{O}). \quad (2)$$

Any increase in T_{ex} of the corresponding levels due to higher excitation (i.e. higher $n(\text{H}_2)$, T_{kin}) is approximately compensated by a loss of level population of the corresponding states to higher states in the J ladder; this is why Eq. 2 holds even if the $J = (2 - 1)$ line is subthermally excited. An unknown quantity in Eq. 2 is the relative abundance of the CO isotopomers studied. For Galactic disk molecular clouds, a CO abundance of $8 10^{-5}$ is frequently assumed (Frerking et al. 1982). Toward the centers of spiral galaxies, metallicities are typically higher by a factor of two than in the local disk (see Vila-Costas & Edmunds 1992). On the other hand in the centers of galaxies the amounts of carbon in the form of CI and CO may be comparable (Gerin & Phillips 2000, Israel & Baas 2002). It is therefore plausible to expect for the galaxies studied here a global CO/H_2 abundance similar to the Galactic disk value, with an uncertainty which could be a factor of two in either direction.

Model calculations suggest that CO isotopomers are not very greatly affected by selective dissociation (Chu & Watson 1983, Glassgold et al. 1985). A fractionation of ^{13}CO via the reaction



(Watson 1976) becomes significant only for kinetic temperatures smaller than 35 K (e.g. Langer et al. 1984). As long as the kinetic temperatures of the CO emitting gas are higher than this it is safe to assume that fractionation of ^{13}CO introduces an error of the H_2 column density which is negligible in comparison to the uncertainty of the CO/H_2 abundance.

The $^{12}\text{C}/^{13}\text{C}$ and $^{16}\text{O}/^{18}\text{O}$ ratios have been determined to be 50 and 200 (Henkel & Mauersberger 1993, Weiß et al. 2001b) in the galaxies studied. Eq. (1) transforms into $N(\text{H}_2) = 1.3 \cdot 10^{21} \text{ cm}^{-2} I(\text{C}^{18}\text{O})$ and $N(\text{H}_2) = 3.3 \cdot 10^{20} \text{ cm}^{-2} I(^{13}\text{CO})$. We have used the latter equation together with our measurements of the $^{13}\text{CO } J = 2 - 1$ line to determine the beam averaged H_2 column densities summarized in Table 4. If the ^{13}CO lines are slightly optically thick, the $N(\text{H}_2)$ values may be higher (see below). While C^{18}O lines could be an even more accurate tracer of $N(\text{H}_2)$, such lines are substantially weaker and are difficult to detect with a proper signal-to-noise ratio.

A comparison between the derived H_2 column densities and $^{12}\text{CO } J = 1 - 0$ measurements (accounting for different spatial resolutions, see Sect 3.3) towards NGC 253 (Houghton et al. 1997, Sorai et al. 2000) and IC 342 (Crosthwaite et al. 2001, Meier & Turner 2001) shows, that a conversion factor X_{CO} which is a factor of 3 – 5 smaller than the Galactic value of $2.3 \cdot 10^{20} \text{ cm}^{-2} (\text{K km s}^{-1})^{-1}$ (Strong et al. 1988) is appropriate for starburst nuclei. This is in line with recent determinations of X_{CO} in M 82 (Weiß et al. 2001b).

4.3. $n(\text{H}_2)$ and CS abundance

We now use the intensity of the CS (5 – 4) lines given in Table 3 to complement the multilevel studies in Mauersberger & Henkel (1989). The levels corresponding to this transition need an H_2 density $\sim 10^4 \text{ cm}^{-3}$ to be excited. We used the large velocity gradient (LVG) code described in Mauersberger & Henkel (1989) to investigate the H_2 density, the CS column density and relative abundance ($n(\text{H}_2)$, $N(\text{CS})$ and $X(\text{CS})=N(\text{CS})/N(\text{H}_2)$). Note that the values given below for $X(\text{CS})$ are beam averaged values for the CS emitting dense gas component (the LVG code gives the source averaged $N(\text{CS})$ which can be multiplied with the beam filling factor, given by a comparison of the code's results with the observed intensities, to obtain the beam averaged $N(\text{CS})$). Any lack of CS emission in the intercloud component due to a low abundance or insufficient excitation increases the local abundance in the CS emitting component. LVG models were calculated for $\log(n(\text{H}_2)) = 2.0$ to 6.0 in steps of 0.2 and $\log(X(\text{CS})/\text{grad}(v)) = -11.7$ to -6.7 in steps of 0.2. The relative abundance $[\text{CS}]/[\text{C}^{34}\text{S}]$ was fixed to 25, the Galactic $^{32}\text{S}/^{34}\text{S}$ abundance ratio (Chin et al. 1996). Since the kinetic temperature of the gas is high (see the results in Sect. 4.1) and the excitation of CS does only weakly depend on T_{kin} for temperatures above 30 K (see e.g. Mauersberger & Henkel 1989) we fixed T_{kin} to 60 K.

Solutions were selected by comparing all beam corrected CS and C^{34}S line intensity ratios derived from Table 3 to the corresponding LVG line intensity ratios using a χ^2 -test. Only those solutions were permitted where the beam averaged H_2 column densities were not below the values derived from our $^{13}\text{CO } J = 2 - 1$ measurements (NGC 253 and IC 342).

For Maffei 2, our non-detection of the $J=5-4$ line and the intensity of the $J=3-2$ CS line detected by Mauersberger et al. (1989a) do not permit a reliable determination of $n(\text{H}_2)$. For IC 342 all observed line intensities can be fitted simultaneously by the LVG models. We derive a moderate $n(\text{H}_2)$ density of $10^{3.9 \pm 0.3} \text{ cm}^{-3}$. The beam averaged CS column density is between $1 \cdot 10^{13} \text{ cm}^{-2}$ and $6 \cdot 10^{13} \text{ cm}^{-2}$. Using the H_2 column density given in Table 4 this corresponds to a beam averaged relative CS abundance of $10^{-8.4 \pm 0.5}$. From an HCN multilevel study Paglione et al (1997) estimated elevated kinetic temperatures and densities toward IC 342 which are consistent with our models. Using more transitions of HCN, Schulz et al. (2001) point out that 5% of the dense gas might have densities of 10^6 cm^{-3} and might be as cool as 30 K.

For NGC 253 and M 82 not all observed line intensities can be fitted by the LVG models simultaneously. As discussed in Mauersberger & Henkel (1989) for NGC 253 this indicates, that the lower transitions of CS arise from a lower density component containing dense concentrations traced by the 5 – 4 transition. This explanation is supported by the LVG solutions we obtain when we do not include either the CS $J = 2 - 1$ or CS $J = 3 - 2$ transition: for NGC 253 we obtain $n(\text{H}_2) = 10^{4.2 \pm 0.7} \text{ cm}^{-3}$ (using CS $J = 2 - 1$, CS $J = 5 - 4$ and $\text{C}^{34}\text{S } J = 2 - 1$) and $n(\text{H}_2) = 10^{4.5 \pm 0.8} \text{ cm}^{-3}$ (using CS $J = 3 - 2$, CS $J = 5 - 4$ and $\text{C}^{34}\text{S } J = 2 - 1$). Including only the low J transitions yields $n(\text{H}_2) = 10^{3.7 \pm 0.6} \text{ cm}^{-3}$. The beam averaged CS column density is between $2 \cdot 10^{13} \text{ cm}^{-2}$ and $2 \cdot 10^{14} \text{ cm}^{-2}$. The beam averaged CS abundance therefore is $10^{-8.4 \pm 0.5}$. Our density estimates are consistent with multilevel studies of HCN (Paglione et al. 1997), HC_3N (Mauersberger et al. 1990), CH_3CN and CH_3CCH (Mauersberger et al. 1991).

The corresponding results for M 82 are: $n(\text{H}_2) = 10^{3.9 \pm 0.7} \text{ cm}^{-3}$ (using CS $J = 2 - 1$, CS $J = 5 - 4$, $\text{C}^{34}\text{S } J = 2 - 1$, and $\text{C}^{34}\text{S } J = 3 - 2$) and $n(\text{H}_2) = 10^{4.2 \pm 0.3}$ (using CS $J = 3 - 2$, CS $J = 5 - 4$ and $\text{C}^{34}\text{S}, J = 2 - 1$ and $\text{C}^{34}\text{S } J = 3 - 2$). The density is not well constrained using the low J lines only. LVG solutions then cover a density range from $n(\text{H}_2) = 10^{3.3}$ to $10^{5.5} \text{ cm}^{-3}$ and low H_2 densities are associated with high 'local' CS abundances and vice versa. Interestingly, solutions are only permitted for $T_{\text{kin}} < 25 \text{ K}$. Beam averaged CS column densities including the CS $J = 5 - 4$ line are in the range between $1 \cdot 10^{13} \text{ cm}^{-2}$ and $6 \cdot 10^{14} \text{ cm}^{-2}$. The beam averaged CS abundance is $10^{-7.9 \pm 0.8}$. The LVG results are summarized in Table 4. Our density estimates are consistent with those from HCN (Paglione et al. 1997) and CH_3CCH (Mauersberger et al. 1991).

Table 4. Physical parameters in the central regions ($\sim 35''$) of nearby galaxies

Source	D	$35''$ equiv. beam size	$N(\text{H}_2)^a$	$\log n(\text{H}_2)$	T_{rot}	$N(\text{NH}_3)$	$N(\text{CS})$	$\log(X(\text{NH}_3))$	$\log(X(\text{CS}))$
	Mpc	pc	10^{21} cm^{-2}	cm^{-3}	K	10^{13} cm^{-2}			
NGC 253	2.5^b	420	17.4	4.2 ± 1.1	100...142	37(7)	2 – 20	-7.7(0.3)	-8.4 ± 0.5
Maffei 2	2.5^c	420	4.6		48, 132	8.6(1.3)		-7.7(0.3)	
IC 342	1.8^d	300	5.7	3.9 ± 0.3	53, 443	7.5(.5)	1 – 6	-7.9(0.3)	-8.4 ± 0.5
M 82	3.9^e	660	9.7	4.3 ± 1.0	29^f	$1.0(.3)^f$	1 – 60	-9.0(0.3)	-7.9 ± 0.8

a) from our $^{13}\text{CO } J = 2 - 1$ data; the uncertainty is a factor of 2 in both directions. b) Mauersberger et al. 1996a; c) Karachentsev et al. 1997; d) McCall 1989; e) Sakai & Madore 1999; f) Weiß et al. 2001b

Table 5. Masses and NH_3 abundances of the warm (≥ 150 K) gas component

	M_{warm}^a	M_{total}^b	$\frac{M_{\text{warm}}}{M_{\text{total}}}$	$\log X(\text{NH}_3)^c$
	$10^6 M_{\odot}$			
NGC 253	2.5	75	0.03	-6.1
IC 342	1.3	13	0.10	-7.5
M 82	75^d	100	$0.2 \dots 0.8^d$	< -9
GC ^e			0.3	$\gtrsim -7$

a) Within a $14'' \times 27''$ aperture, from Rigopoulou et al (2002) scaled to the distances in Table 4

b) from ^{13}CO data in this paper, the uncertainty is a factor of 2

c) The warm NH_3 relative to the warm H_2

d) It is unknown to us to which pointing position and orientation of the ISO beam in Rigopoulou et al. (2002) the mass in Col. 2 refers; therefore the large uncertainty of Col. 4

e) Rodríguez-Fernández et al. (2001)

4.4. Origin and heating of the warm gas

In the complex environment of the central few 100 pc of an active galaxy there are certainly several coexisting gas components. Transitions from molecules with a high dipole moment such as ammonia and CS need a density $\sim 10^4 \text{ cm}^{-3}$ to be excited, in contrast to CO lines which need a few 100 cm^{-3} . Our ammonia Boltzmann plots also suggest that there are several components with different temperatures within our beams. This is also what we observe toward the central region of our Galaxy (Hüttemeister et al. 1993b). The relative abundances of the high density tracers NH_3 and CS in Table 4 are from a comparison with the total molecular column densities derived from ^{13}CO ; they are therefore an average over all gas components. We can, however, estimate the relative abundance of warm ammonia in the gas component where it probably arises. This component is traced by rotational quadrupole transitions of H_2 , e.g. the $0 - 0 S(0)$ line, the upper level of which is 510 K above the ground state. From such lines masses of warm gas with a temperature of ~ 150 K have been recently determined by Rigopoulou et al. (2002) for a number of starburst and Seyfert galaxies. We have scaled the masses quoted in Rigopoulou et al. (2002) to the distances used here and list them in Table 5. When we compare the masses of warm H_2 toward M 82, IC 342, NGC 253 with the total H_2 masses from our ^{13}CO

data and also take into account Galactic Center H_2 measurements obtained by Rodríguez-Fernández et al. (2001) it turns out that the warm gas makes up a substantial fraction of the total gas mass in the centers of nearby starburst galaxies and our own Galaxy. We cannot confirm, however, the claim by Bradford et al. (2002) that *all* the gas traced by CO is warm (and, hence, requires a uniformly heating source such as cosmic rays) since this would lead to contradicting H_2 mass estimates from observations of H_2 and CO.

Newly formed high mass stars may heat only very localized regions via dust absorption. Even in the central regions of luminous galaxies, global dust temperatures rarely exceed 50 K (e.g. Henkel et al. 1986). In the case of NGC 253, the central mid-infrared emission comes mainly from cold (23 K) dust; only a small fraction, $\ll 20\%$ of the dust mass has temperatures similar to 148 K (Melo et al. 2002). Possible mechanisms capable of elevating the H_2 temperature to global values of 100 K and more over an extent of several 100 pc are shocks, which may result e.g. from the dissipation of tidal motions, photodissociation and irradiation by X-rays (see e.g. Rigopoulou et al. 2002). Other possible heating mechanisms involve cosmic rays (Güsten et al. 1981, Farquhar et al. 1994) or a magnetic ion-slip process (Scalo 1977).

In the central regions of IC 342 and NGC 253, the relative abundance of the hot ammonia to the hot H_2 component is elevated over the relative ammonia abundances observed also including the cold component. In NGC 253 a value of 10^{-6} is reached, which is similar to values found in Galactic hot cores (e.g. Hüttemeister et al. 1993b) and the central region of the Milky Way (Rodríguez-Fernández et al. 2001). The high NH_3 abundances in these galaxies and presumably also in Maffei 2 exclude heating mechanisms, such as photo-ejection from grains (Genzel et al. 1984), capable of destroying this fragile molecule which has a dissociation energy of only 4 eV. NH_3 has been observed, with a similar abundance as in the warm components of NGC 253 and IC 342, in Wolf Rayet environments (Rizzo et al. 2001), which can be explained by a release of NH_3 from dust grains facilitated by weak shocks from the expansion of the bubble created by the stellar wind. C-shocks have also to be used to explain the abundance of complex molecules and the heating in the central region of our Galaxy (Flower et al. 1995, Martín-Pintado et al. 2001). Such intermittent shocks, created by frequent cloud-cloud

collisions can also explain the temperature gradients seen in the NH_3 data. Cosmic rays can also heat large volumes of gas to high temperatures

It is interesting that the warm gas fraction seems to be highest in M82 where no warm ammonia component has been detected. Here the relative ammonia abundance in the hot gas component must be $< 10^{-9}$. This indicates that NH_3 traces a different molecular gas component in M82 than in NGC 253, Maffei 2 and IC 342. For M82, the presence of an intense dissociating radiation field and the predominance of warm molecular filaments with low H_2 column density and density (Mao et al. 2000) do not only explain the low abundance of NH_3 (see e.g. the model in Fuente et al. 1993) and other complex molecules but also the excitation of CO rotational levels (Weiß 2001b) in the warm H_2 gas detected by Rigopoulou et al. (2002). One could argue that larger quantities of warm NH_3 exist in this low density gas, but are escaping from being detected due to lacking excitation. This is, however, improbable since NH_3 molecules with their low dissociation energy would be rapidly destroyed by the interstellar radiation field in a low H_2 density and column density environment.

The low NH_3 abundance contrasts with a CS abundance which is normal or even slightly higher than in other galaxies. Chemical models of photon dominated regions (PDR) show that at moderate extinctions of 6–8 mags., CS is strongly enhanced up to values of more than 10^{-6} due to the presence of a small amount of ionized sulphur (Sternberg & Dalgarno 1995). The bulk of the CS we are seeing in M82 might come from such moderately shielded regions.

The lack of ammonia in the warm phase of M82 also suggests that the overall heating mechanism for the molecular gas is different. In a starburst, photo-dissociating radiation is capable of heating a large fraction of the gas to 150 K (e.g. Rodríguez-Fernández et al. 2001). The low abundance of ammonia toward M82, the properties of the CO emission (Mao et al. 2000) and the detection of abundant emission of HCO (García-Burillo et al. 2002), a tracer of photo-dissociation regions, indicates that PDRs are the main heating source that also have influenced the chemistry of the bulk of the circumnuclear gas in this galaxy. In regions where the CS abundance is enhanced, shielding may be sufficient to prevent the heating of the CS emitting gas to high kinetic temperatures.

5. Conclusions

The main conclusions of this paper are:

1. Our detections of highly excited lines of ammonia toward the nuclear regions of three nearby galaxies reveal the presence of gas components as warm as 50 K ... 440 K toward Maffei 2, IC 342 and NGC 253. Part of the gas may be cooler (~ 50 K). These temperatures resemble values observed toward the central region of our own Galaxy.
2. The global beam averaged relative ammonia abundances toward NGC 253, Maffei 2 and IC 342 are with (3.3 ... 5.7) 10^{-8} remarkably similar. The NH_3 abundances in

the warm ($\gtrsim 150$ K) phase in those galaxies, and also in the central region of the Milky Way, are $\sim 10^{-7}$. Toward M82 this abundance is lower by more than an order of magnitude.

3. Toward NGC 253, IC 342 and M82 an elevated H_2 density of $\sim 10^4 \text{ cm}^{-3}$ is estimated from multilevel studies of CS.

4. The rich chemistry and high ammonia abundances observed in NGC 253, Maffei 2, IC 342 and the Galactic central region may be in part explained by evaporation from the ice mantles of interstellar dust grains due to C-shocks. These shocks would also provide the heating to the observed elevated temperatures.

5. In the central region of M82, photodissociating radiation can explain the high temperature of H_2 , the lack of ammonia and other complex molecules in M82, and the high abundance of CS and HCO.

Acknowledgements. We thank Drs. David Meier and Jean Turner for making available their $^{13}\text{CO } J = 1 - 0$ data to us. Dr. R. Peng made available in digital form their CS data toward NGC 253. We thank the staff at the Effelsberg 100-m telescope and the Heinrich-Hertz 10-m sub-mm telescope for their valuable support during the observations and wish to thank an anonymous referee for constructive criticism that helped to improve the article.

References

- Baan, W. A., Henkel, C., Schilke, P., Güsten, R. & Mauersberger, R. 1990, ApJ, 353, 132
- Baars, J. W. M. & Martin, R. N. 1996, Rev. Mod. Astr., 9, 111
- Bloemen, J. B. G. M., Strong, A. W., Mayer-Hasselwander, H. A., et al. 1986, A&A, 154, 25
- Bradford, C. M., Nikola, T., Stacey, G. J., et al. 2002, BAAS, 201, 2607
- Brouillet, N. & Schilke, P. 1993, A&A, 277, 381
- Ceccarelli, C., Baluteau, J.-P., Walmsley, C. M., et al. 2002, A&A, 383, 603
- Chin, Y.-N., Henkel, C., Whiteoak, J. B., Langer, N. & Churchwell, E. B. 1996, A&A, 305, 960
- Chu, Y.-H. & Watson, W. D. 1983, ApJ, 267, 151
- Combes, F. 1991, ARA&A, 29, 195
- Crosthwaite, L. P., Turner, J. L., Hurt, R. L., et al. 2001, AJ, 112, 797
- Dahmen, G., Hüttemeister, S., Wilson, T. L. & Mauersberger, R. 1998, A&A, 331, 959
- Dickman, R. L. 1975, ApJ, 202, 50
- Dickman, R. L., Snell, R. L. & Schloerb, F. P. 1986, ApJ, 309, 326
- Downes, D., Radford, S. J. E., Guilloteau, S., et al. 1992, A&A, 262, 424
- Downes, D. & Solomon, P. M. 1998, ApJ, 507, 615
- Dumke, M., Nietten, Ch., Thuma, G., Wielebinski, R. & Walsh, W. 2001, A&A, 373, 853
- Farquhar, P. R. A., Millar, T.J. & Herbst, E. 1994, MNRAS, 269, 641
- Flower, D. R., Pineau des Forêts, G. & Walmsley, C. M. 1995, A&A, 294, 815
- Frerking, M. A., Langer, W. D. & Wilson, R. W. 1982, ApJ, 262, 590

- Fuente, A., Martín-Pintado, J., Cernicharo, J. & Bachiller, R. 1993, *A&A*, 276, 473
- García-Burillo, S., Martín-Pintado, J., Fuente, A., Usero, A. & Neri, R. 2002, *ApJ*, 575, L55
- Genzel, R., Watson, D. M., Townes, C. H., et al. 1984, *ApJ*, 276, 551
- Gerin, M. & Phillips, T. G. 2000, *ApJ*, 537, 644
- Glassgold, A. E., Huggins, P. J. & Langer, W. D. 1985, *ApJ*, 290, 615
- Güsten, R. 1989, in *The Center of the Galaxy*, IAU Symp. 136, ed: M. Morris, Kluwer, Dordrecht, p. 89
- Güsten, R., Walmsley, C. M. & Pauls, T. 1981, *A&A*, 103, 197
- Güsten, R., Serabyn, E., Kasemann, C., et al. 1993, *ApJ*, 402, 537
- Harrison, A., Henkel, C. & Russell, A. 1999, *MNRAS*, 303, 157
- Henkel, C. & Mauersberger, R. 1993, *A&A*, 274, 730
- Henkel, C., Wouterloot, J. G. A. & Bally, J. 1986, *A&A*, 155, 193
- Henkel, C., Mauersberger, R., Peck, A. B., Falcke, H. & Hagiwara, Y. 2000, *A&A*, 361, L45
- Houghton, S., Whiteoak, J. B., Koribalski, B., et al. 1997, *A&A*, 325, 923
- Hüttemeister, S., Mauersberger, R. & Henkel, C. 1997, *A&A*, 326, 59
- Hüttemeister S., Wilson, T. L., Bania, T. M. & Martín-Pintado, J. 1993a, *A&A*, 280, 255
- Hüttemeister, S., Wilson, T. L., Henkel, C. & Mauersberger, R. 1993b, *A&A*, 276, 445
- Hüttemeister, S., Wilson, T. L., Mauersberger, R., Lemme, C., Dahmen, G. & Henkel, C. 1995, *A&A*, 294, 667
- Israel, F. P. & Baas, F. 2002, *A&A*, 383, 82
- Jackson, J. M., Paglione, T. A. D., Carlstrom, J. E. & Rieu, N. 1995, *ApJ*, 438, 695
- Jog, C. J. & Das, M. 1993, *Evolution of Galaxies and their Environment*, NASA AMES, p. 155
- Karachentsev, I., Drozdovsky, I., Kajsin, S. et al., 1997 *A&AS*, 124, 559
- Langer, W. D., Graedel, T. E., Frerking, M. A. & Armentrout, P. B. 1984, *ApJ*, 277, 581
- Mao, R. Q., Henkel, C., Schulz, A., et al. 2000, *A&A*, 358, 433
- Martin, R. N. & Ho, P. T. P. 1986, *ApJ*, 308, L7
- Martín-Pintado, J., Rizzo, J. R., de Vicente, P., Rodríguez-Fernández, N. J. & Fuente, A. 2001, *ApJ*, 548, L65
- Mauersberger, R. & Henkel, C. 1989, *A&A*, 223, 79
- Mauersberger, R. & Henkel, C. 1993, *Rev. Mod. Astron.*, 6, 69
- Mauersberger, R., Wilson, T. L., Walmsley, C. M., Henkel, C. & Batrla, W. 1985, *A&A*, 146, 168
- Mauersberger, R., Henkel, C., Wilson, T. L. & Walmsley, C. M. 1986, *A&A*, 162, 199
- Mauersberger, R., Wilson, T. L. & Henkel, C. 1988, *A&A*, 201, 123
- Mauersberger, R., Henkel, C., Wilson, T.L. & Harju, J. 1989, *A&A*, 226, L5
- Mauersberger, R., Henkel, R. & Sage, L. J. 1990, *A&A*, 236, 63
- Mauersberger, R., Henkel, C., Walmsley, C. M., Sage, L. J. & Wiklind, T. 1991, *A&A*, 247, 307
- Mauersberger, R., Wilson, T. L., Mezger, P. G., Gaume, R. & Johnston, K. J. 1992, *A&A*, 256, 640
- Mauersberger, R., Henkel, C. & Chin, Y.-N. 1995, *A&A*, 294, 23
- Mauersberger, R., Henkel, C., Wielebinski, R., Wiklind, T. & Reuter, H.-P. 1996a, *A&A*, 305, 421
- Mauersberger, R., Henkel, C., Whiteoak, J. B., Chin, Y.-N. & Tieftrunk, A. R. 1996b, *A&A*, 309, 705
- Mauersberger, R., Henkel, C., Walsh, W. & Schulz, A. 1999, *A&A*, 341, 256
- McCall, M. L. 1989, *AJ*, 97, 1341
- Meier, D. S., Turner, J. L., Hurt, R. L. 2000, *ApJ*, 531, 200
- Meier, D. S. & Turner, J. L. 2001, *ApJ*, 551, 687
- Melo, V. P., Pérez García, A. M., Acosta-Pulido, J. A., Muñoz-Tuñón, C. & Rodríguez Espinosa, J. M. 2002, *ApJ*, 574, 709
- Ott, M., Witzel, A., Quirrenbach, A., et al. 1994, *A&A*, 284, 331
- Paglione, T. A. D., Jackson, J. M., Ishizuki, S. & Rieu, N. 1995, *AJ*, 109, 1716
- Paglione, T. A. D., Jackson, J. M. & Ishizuki, S. 1997, *ApJ*, 484, 656
- Peng, R., Zhou, S., Whiteoak, J. B., Lo, K. Y. & Sutton, E. C. 1996, *ApJ*, 470, 821
- Rigopoulou, D., Kunze, D., Lutz, D., Genzel, R. & Moorwood, A. F. M. 2002, *A&A*, 389, 374
- Rizzo, J. R., Martín-Pintado, J. & Henkel, C. 2001, *ApJ*, 553, L181
- Rodríguez-Fernández, N. J., Martín-Pintado, J., Fuente, A., et al. 2001, *A&A*, 365, 174
- Sakai, S. & Madore, B.F. 1999, *ApJ*, 526, 599
- Sanders, D. B., Scoville, N. Z. & Solomon, P. M. 1985, *ApJ*, 289, 373
- Scalo, J. 1977, *ApJ*, 213, 705
- Schulz, A., Güsten, R., Köster, B. & Krause, D. 2001 *A&A*, 371, 25
- Seaquist, E. R., Frayer, D. T. & Bell, M. B. 1998, *ApJ*, 507, 745
- Sodroski, T. J., Odegard, N., Dwek, E., et al. 1995, *ApJ*, 452, 262
- Solomon, P. M., Downes, D., Radford, S. J. E. & Barrett, J. W. 1997, *ApJ*, 478, 144
- Sorai, K., Nakai, N., Kuno, N., Nishiyama, K. & Hasegawa, T. 2000, *PASJ*, 52, 785
- Sternberg, A. & Dalgarno, A. 1995, *ApJS*, 99, 565
- Strong, A. W., Bloemen, J. B. G. M., Lebrun, F., et al. 1988, *A&A*, 207, 1
- Takano, S., Nakai, N., Kawaguchi, K. & Takano, T. 2000, *PASJ*, 52, L67
- Takano, S., Nakai, N. & Kawaguchi, K. 2002, *PASJ*, 54, 195
- Vila-Costas, M. B. & Edmunds, M. G. 1992, *MNRAS*, 259, 121
- Walker, C. E., Bash, F. N., Martin, R. N. & Phillips, T. G. 1993, *Rev. Mexicana de Astron. y Astrofis.*, 27, 203
- Walmsley, C. M. & Ungerechts, H. 1983, *A&A*, 122, 164
- Ward, J. S., Zmuidzinas, J., Harris, A. I. & Isaak, K. G. 2001, *BAAS*, 199, 1482
- Watson, W. D., Anicich, V. G. & Huntress, W. T. 1976, *ApJ*, 205, L165
- Weiß, A., Neininger, N., Henkel, C., Stutzki, J. & Klein, U. 2001a, *ApJ*, 554, L143
- Weiß, A., Neininger, N., Hüttemeister, S. & Klein, U. 2001b, *A&A*, 365, 571
- Young, J. S. & Scoville, N. Z. 1991, *ARA&A*, 29, 581